TECHNICAL MEMORANDUMS

NATIONAL ADVISORY COMMITTEE FOR AERONAUTICS

No. 814

EXPERIMENTAL STUDIES OF THE EFFECTIVE WIDTH OF BUCKLED SHEETS

By R. Lahde and H. Wagner

Luftfahrtforschung
Vol. 13, No. 7, July 20, 1936
Verlag von R. Oldenbourg, München and Berlin

Washington
December 1936

NATIONAL ADVISORY COMMITTEE FOR AERONAUTICS

TECHNICAL MEMORANDUM NO. 814

EXPERIMENTAL STUDIES OF THE EFFECTIVE WIDTH OF BUCKLED SHEETS

By R. Lahde and H. Wagner

SUMMARY

Airplane design makes frequent use of thin sheet metal or plywood shells which buckle under shear and compression stresses, although some support is given at the point where sheet and angles join. So far as it deals with the absorption of compressive stresses this fact is allowed for in the calculation by introducing a participating stress bearing or "effective width", i.e., a part of the sheet section of certain width is allocated to the section of the edge stiffener.

The object of the present experiments is a more exact determination of the effective width for the case of pure compression and of the sheet clamped at the angle section. From the experimental data on the effective width the calculation of the buckling load of an angle joined to a thin sheet is then deduced. The experimental results for simultaneous appearance of transverse forces in the buckled sheet (tension fields) are reserved for a continuation of this article in a subsequent issue.

INTRODUCTION

No direct elongation measurements were effected on the experimental sheets themselves by the test method employed in the determination of the "effective width"** although we did measure the elongation and spacing of the

---

*"Versuche zur Ermittlung der mittragenden Breite von verbeulten Blechen." Luftfahrtforschung, vol. 13, no. 7, July 20, 1936, pp. 214-223.

**This "effective width" in the buckled sheet has absolutely nothing to do with the much discussed effective width at the point of load applications.

two angle sections of the specimen sheet. The inclinations of the sheet caused on the experimental sheet itself as a result of buckling were determined by a special instrument.

Therefrom we computed:

1) The flexural stresses,

2) The mean compressive stress of every strip running in the direction of the compressive stress, that is, the mean compressive stress distribution over the sheet width, and from it the "effective width",

3) The mean axial stress transverse to the compressive direction.

A slight transgression of the buckling load is followed by sinusoidal folds or wrinkles in longitudinal direction. But when the stress in the angles exceeds more than about 20 times the buckling stress of the sheet, the edge manifests intermediate wrinkles (fig. 1).

The most important results of the experiments are the following:

Let σ_k be the stress in the angle section at buckling of the sheet, and σ the ultimate stress in the angle (after buckling). The compressive load P carried by the sheet then increases beyond the buckling load P_k of the sheet. By a slight overstepping of the buckling load (up to about $\frac{\sigma}{\sigma_k} = 3$), the formula

$$P = P_k \sqrt{\frac{\sigma}{\sigma_k}} \tag{1a}$$

yields correct values for P, while for considerable excess beyond buckling load the formula

$$P = k P_k \sqrt{\frac{\sigma}{\sigma_k}} \tag{1b}$$

is applicable. (The experimental values k are shown in figure 2; k finally increases to 2.)

Equation (1a) is retained for sheets restrained at the edge. As regards sheets freely supported at the edge, Schnadel's calculations (reference 1) reveal that (1a) is applicable also when the excess is small. Moreover, in this case it may be expected that the load supported by the sheet is higher than given in (1a) by considerably exceeded buckling load. These facts would seem to suggest that equation (1a) is for any possible case a safe measure of the load supported by the sheet.

The stress σ_k as well as the buckling load P_k depend upon whether the compression of the edge stiffeners bounding the sheet is accompanied by a change $e_y t$ in its spacing or distance t. Figure 3 gives σ_k against $\frac{e_y}{e_x}$*, with e_x denoting the temporary specific compression of the angle sections $\left(\text{that is, } e_x = \frac{\sigma}{E}\right)$. The buckling load P_k of the sheet follows from the stress σ_k in the angles at:

$$P_k = \sigma_k \, t \, s \, \frac{1 + \nu \frac{e_y}{e_x}}{1 - \nu^2}$$

ν = Poisson's ratio $\left(\nu = \frac{1}{3}\right)$.

In airplane design it is customary, when determining the stress set up by a given compression in the angle, to allow for the load quota of the sheet by an effective width b_m. The experimental k values of figure 2 permit the calculation of this width

$$b_m = 0.5 \, k \, t \sqrt{\frac{e_k}{e_x}} \, \frac{1 + \nu \frac{e_y}{e_x}}{1 - \nu^2}$$

---

*The curves were taken from the report: "Über Konstruktions-und Berechnungsfragen des Blechbaues" by Herbert Wagner, V.G.L. Yearbook, 1928. The curve for clamped sheets was corrected by several points computed according to Reissner's method.

of the particular strip on each side of the profile (see fig. 5 for example).

For the case of the sheet clamped at the edge and constant spacing of angles ($e_y = 0$) the present experiments disclose

$$b_m = 1.2\ k\ \frac{s}{\sqrt{e_x}}\ *$$

For sheet clamped at the edge and any given variation in spacing of the edge stiffeners it is

$$b_m = b\ \frac{1 + \nu \frac{e_y}{e_x}}{1 - \nu^2}$$

whereby $2\ \frac{b}{t}$ is read from figure 4 for rough calculations

$$b_m \approx b$$

is acceptable.

Moreover, the value $\frac{2\ b}{t}$ of figure 4 is approximately applicable to supported sheets.

These data can equally be used for the calculation of the buckling load in a section joined to a thin sheet. The buckling load of an angle depends upon its bending stiffness. The proportion of the sheet on the bending stiffness is governed by the compressive stiffness of the sheet. In the determination of the inertia moment of the angle this is allowed for by the inclusion of a strip of corresponding width b'. For this width b' the experiments for clamped sheets give the value read in figure 4 which, for small transgression of the buckling load at least, is approximately valid even for superposed sheets. The additive sheet area therefore is:

---

*Be it noted that the values b and b_m as shown in figure 5 refer to only one side of the sheet. If the sheet, as in the majority of cases, extends to both sides of the angle, the double value, that is, 2 b and 2 b_m respectively must be employed.

$$t\,s\,\frac{1+\nu\frac{e_y}{e_x}}{1-\nu^2}\,\frac{2b}{t} \qquad (1c)$$

in the determination of the stress in the section, and

$$t\,s\,\frac{1+\nu\frac{e_y}{e_x}}{1-\nu^2}\,\frac{2b'}{t} \qquad (1d)$$

in the determination of the inertia moment of the section.

RESULTS

Visualize a flat sheet with an angle (section), both sheet and angle being of infinite length. At the edge stiffener itself the sheet is secured against buckling by adequately close rivet pitch or by clamping between two angles.

Now sheet and section are compressed so that both undergo the same amount of shortening. The sheet outside of the edge stiffener buckles as a rule. One piece of the strip I-I of the sheet forms wrinkles whose developed length l_1' though less than the length l of the unstressed section or plate strip, exceeds the length l_1 of the compressed section. This is the reason the mean compressive stress $\overline{\sigma}_x$ of this strip is generally lower than the stress in the section. With increasing distance from the section y the stress in the sheet continues to drop and becomes very low at greater distance. The area below curve $\overline{\sigma}_x = f(y)$, multiplied by the wall thickness s, gives the carrying power of the sheet. The width of the rectangle of equivalent content and height equal to the stress existing in the sheet in compressive direction if the sheet did not buckle, is called the effective width b*.

*The term effective width b was chosen since as regards this b the test data lend themselves to simple representation even by existence of a transverse elongation e_y within the limits of experimental accuracy. At the instant of buckling it is in every case $b = 1/2\ t$. On a previous page the effective width b_m was referred in accord with the hitherto usual, to the stress in the angle section. The equations with this b_m become more complicated by the factor

$$\frac{b_m}{b} = \frac{1+\nu\frac{e_y}{e_x}}{1-\nu^2}$$

Consider the sheet strip of width b held at both edges between sections. The effective width b, (fig. 6) now depends fundamentally on the dimensions of the strip (t, s) and on the shifting of the angle sections, that is, on their compressive elongation e_x* as well as their inevitably different spacing e_y t. The thus defined quantity e_y has the dimension of an elongation.**

Consequently

$$b = F(e_x; e_y; t; s)$$

This type of relationship may be simplified by dimension method (Appendix). It gives

$$\frac{b}{t} = F\left(\frac{e_x}{e_k}; \frac{e_y}{e_x}\right) \tag{2}$$

whereby e_k is that compressive elongation in x direc- at which the sheet buckles. As the buckling elongation is proportional to $\left(\frac{s}{t}\right)^2$, equation (2) may also be written as

$$\frac{b}{t} = F_1\left[e_x\left(\frac{t}{s}\right)^2; \frac{e_y}{e_x}\right] \tag{3}$$

Now the effect of $\frac{e_y}{e_x}$ was, according to our experiments, small within the range usually under consideration (fig. 13). For the case $\frac{e_y}{e_x} = 0$, $\frac{b}{t}$ is only more affected by the amount by which the buckling load is exceeded.

---

*By e_x is meant the mean elongation of the whole sheet in x direction, in contrast to elongation e_x of the separate sheet element in x direction.

**Mutual displacements of both angle sections in longitudinal direction, that is, the appearance of the transverse stresses in the sheet, are disregarded here, as this case is treated in a subsequent report on the same subject.

$$\frac{b}{t} = F\left(\frac{e_x}{e_k}\right) = F_1\left[e_x\left(\frac{t}{s}\right)^2\right] \qquad (3a)$$

Figure 7 shows $\frac{b}{t}$ plotted against the amount by which the buckling load $\frac{e_x}{e_k}$* is exceeded. But when this is quite considerable it is advisable to resort to figure 8.

Figure 8 discloses that for $\frac{e_x}{e_k} > 3$ the effective width b is computable with sufficient accuracy from

$$\frac{b}{t} = 2.1\sqrt{\left(\frac{s}{t}\right)^2\frac{E}{\sigma}} - 3.7\left(\frac{s}{t}\right)^2\frac{E}{\sigma} \qquad (4)$$

This relation (dashed line) is shown in all diagrams. It always runs along the lower boundary of the test points.

It is probable that when $\frac{e_x}{e_k}$ increases the value $\frac{b}{s}\sqrt{e_x}$ approaches a fixed limiting value which, after extrapolation, would give 2.22. In view of this, the function $\frac{b}{s}\cdot\sqrt{e_x} = 2.2$ is shown as asymptote in dash-dots in the diagrams.

Once the buckling load has been exceeded, the effective width b diminishes quite rapidly, according to figure 7. Nevertheless, the load taken up by the sheet continues to increase with increasing stress.

Figure 9 shows the load supported by the sheet in comparison to the load carried at buckling; that is, value $\frac{P}{P_k}$ against the amount of exceeded buckling load.

Figure 10 illustrates the (mean) compressive stress plotted against the width of the sheet strip for varyingly exceeded buckling load. It is noted that at $\frac{e_x}{e_k} > 50$,

---

*Here e_k is the theoretical buckling elongation which for $e_y = 0$ yields $e_k = 4.78\left(\frac{s}{t}\right)^2$. The experimental curves are, so far as this is possible with the unavoidable irregularities of test sheets, in agreement with this figure.

contribution of the middle part of the sheet to compression is most likely at an end, and at any further increase of $\frac{e_x}{e_k}$ the effective width b probably becomes unaffected by the stiffeners. This would be identical with the above voiced conjecture according to which $\frac{b}{s}\sqrt{e_x}$ tends toward a fixed limiting value when $\frac{e_x}{e_k}$ increases.

Cumulative with the compressive stress in the edge stiffener is the flexural stress due to buckling. The resultant bending compressive stress always becomes maximum at a certain distance from the angle section, as seen in figure 11. By minor overstepping of the buckling load, this maximum lies in the center of the strip; by more marked overstepping, it is closer to the edge. Then the resulting compression-bending stress is lower again in the center and becomes, in the extreme case of infinitely exceeding the buckling load $\left(\frac{e_k}{e_x} = 0\right)$, equal to zero. It is only when the buckling load is slightly exceeded that the resultant stress of the sheet lies substantially (80 percent) above the stress in the angle section. Consequently, if the sheet possesses precisely a value of $\frac{t}{s}$, so that it buckles a little prior to reaching the yield point, it is almost simultaneously followed by an appreciable stress above the yield point, and a large portion of the sheet loses its capacity of support unless the sheet is so thin that it buckles substantially before the yield point in the angles has been reached - in which case the resultant stress in the sheet is then only slightly higher than the stress in the edge stiffeners, up to near the yield point.

The mean stresses transverse to the compression direction $\overline{\sigma}_y$ were also computed. Figure 12 illustrates the ratio of this stress to the stress σ_{x_B} existing in the assumedly nonbuckled sheet versus $\frac{e_x}{e_k}$. Here the scatter of the test points is comparatively greater on account of the small absolute quantity of this stress. However, the measurements reveal a compressive stress of the magnitude of $\overline{\sigma}_y = \nu\,\sigma_{x_B}$ in transverse direction at the very instant of buckling, and a rapid drop in this compression as $\frac{e_x}{e_k}$ increases. High values of $\frac{e_x}{e_k}$ are accompanied by transverse tension stresses $\overline{\sigma}_y$ of the order of magnitude of $0.08\,\sigma_{x_B}$.

All test data so far refer to the case that no mutual displacement of the clamping rails occurs transverse to the direction of loading ($e_y = 0$) which, in fact, was practically realized in the majority of the tests. But for checking the effect of $\frac{e_y}{e_x}$, the tests were made with artificially produced transverse shifting of the cheeks and the results plotted in figure 13. The discrepancies of the points from the tests without transverse elongation (heavy line) lie almost within experimental accuracy.

This means that the test data for the experiments without transverse elongation are equally applicable - and with practically sufficient accuracy - to cases of any transverse elongation within the range $0.4 > \frac{e_y}{e_x} > -1$ and, particularly, for the case of compression members freely displaceable in transverse direction ($\sigma_y = 0$). Even the curves (figs. 7, 8, and 9, as well as fig. 2) have this general validity when the quantities $\frac{b}{t}$, $\frac{e_x}{e_k}$, $\frac{P}{P_k}$, or the particular given functions of only these quantities are utilized as coordinates.

On the other hand, the test series of the five points with the highest figures would make it appear that in this range a positive transverse elongation $\left(\frac{e_y}{e_x} \text{ negative}\right)$ induces a slight increase in effective width b. Experiments with greater compressive elongation in transverse direction were omitted because of the very irregular wrinkling. Figure 14 shows the ratio of buckle length d in sheet center to sheet width t versus $\frac{e_x}{e_k}$.

CALCULATION OF BUCKLING LOAD OF EDGE STIFFENERS

The buckling load Q_k of an angle section riveted to a thin sheet wall depends upon its bending stiffness. The width of the sheet strip, which may be considered by the determination of inertia moment I, is governed by the compressive stiffness $\frac{\partial P}{\partial e_x}$ of the sheet. The width of this strip must be well differentiated from the effective width b as regards load absorption. Both widths have one thing in common: Both are dependent on the stress and on $\frac{e_x}{e_k}$.

The calculation of the compressive stiffness of the sheet proceeds from (equation 1b):

$$P = k\, P_k \sqrt{\frac{e_x}{e_k}}$$

whereby

$$P_k = t\ s\ E\ e_k\ \frac{1 + \nu\ \frac{e_y}{e_x}}{1 - \nu^2}$$

This term must be differentiated according to e_x. The result will depend upon the mean elongation transverse to the compressive direction e_y, when e_x changes. And that is a question of constructive formation not always easy to answer in the individual case.

We shall consider two extreme cases, which cover most of the cases encountered in practice:

On reaching the buckling load, a deflection of the angle section - that is, a change of e_x in the sheet is:

1) not accompanied by a change in the existing e_y, that is, $\frac{\partial e_y}{\partial e_x} = 0$;

2) accompanied by a change in e_y proportional to e_x, that is, $\frac{\partial\ \frac{e_y}{e_x}}{\partial\ e_x} = 0$.

In the first case, the calculation of the compressive stiffness of the sheet gives:

$$\frac{\partial P}{\partial e_x} = \frac{t\ s\ E}{1-\nu^2}\left[\frac{k}{2}\sqrt{\frac{e_k}{e_x}}\left(1 - \nu\ \frac{e_y}{e_x}\right) - \frac{1}{2}\ \frac{\partial k}{\partial \sqrt{\frac{e_k}{e_x}}}\ \frac{e_k}{e_x}\left(1 + \nu\ \frac{e_y}{e_x}\right)\right] \qquad (5)$$

The stiffness of the sheet being $\frac{t\ s\ E}{1-\nu^2}$ provided it does not buckle under the cited assumptions, the bracketed value represents the reduction in sheet stiffness caused by the buckling.

In the second case it is:

$$\frac{\partial P}{\partial e_x} = t\ s\ E\ \frac{1 + \nu\ \frac{e_y}{e_x}}{1 - \nu^2}\left[\frac{k}{2}\sqrt{\frac{e_k}{e_x}} - \frac{1}{2}\ \frac{\partial k}{\partial\sqrt{\frac{e_k}{e_x}}}\ \frac{e_k}{e_x}\right] \qquad (6)$$

Here the stiffness of the nonbuckling sheet would be $t\ s\ E\ \frac{1 + \nu\ \frac{e_y}{e_x}}{1 - \nu^2}$, and the bracketed term the decrease in stiffness due to buckling.

Now the difference between the two computed bracketed terms disclosed by the factors $1 - \nu\ \frac{e_y}{e_x}$ and $1 + \nu\ \frac{e_y}{e_x}$ is so small by the $\frac{e_y}{e_x}$ occurring in practice as to be negligible in view moreover of the existing scatter of the test data. It is therefore recommended to use in every case the most easily computed value:

$$2\ \frac{b'}{t} = \frac{k}{2}\sqrt{\frac{e_k}{e_x}} - \frac{1}{2}\ \frac{\partial k}{\partial\sqrt{\frac{e_k}{e_x}}}\ \frac{e_k}{e_x}$$

illustrated in figure 4, as basis of the calculation. The values k and $\frac{\partial k}{\partial\sqrt{\frac{e_k}{e_x}}}$ were taken from the curve, figure 2.

When computing the inertia moment I of the whole angle section in case the sheet did not buckle, the value

$$t\ \frac{1 + \nu\ \frac{e_y}{e_x}}{1 - \nu^2}$$

is to be inserted as sheet width. For the buckled sheet a width of sheet strip $t\ \frac{2b'}{t}\ \frac{1 + \nu\ \frac{e_y}{e_x}}{1 - \nu^2}$ is to be inserted (in similar manner as for defining Karman's buckling modulus after exceeding the yield point) and, specifically, both with regard to inertia moment I and the center of

pressure to which this is to be referred.

Summarizing: With Q, the total compression on sheet angle section

F_p, area of angle section, and

$t\ s$, area of sheet belonging to the angle section,

the angle section is subject to a pure compressive stress:

$$\sigma = \frac{Q}{F_p + 2b_m\ s} = \frac{Q}{F_p + 2\ b\ s\ \frac{1 + \nu\ \frac{e_y}{e_x}}{1 - \nu^2}}$$

provided that the effective line of the force Q passes through the common center of pressure of section area and effective sheet area $2b_m\ s$. To check whether or not buckling takes place, the value $2\ \frac{b'}{t}$ (fig. 4) must be determined for this stress σ, or $\frac{\sigma}{\sigma_k}$ or $\frac{e_x}{e_k}$, respectively. As regards the determination of the total inertia moment I, as well as of the center of pressure to which I is to be referred, the sheet area $2b'\ s\ \frac{1 + \nu\ \frac{e_y}{e_x}}{1 - \nu^2}$ is to be inserted.

These arguments apply to sheets clamped at the edge. No experimental data are available for cases in which other buckling conditions existed. Even so, if in such cases the buckling load is known, one is always on the safe side when expressing the load absorption of the sheet with

$$P = P_k \sqrt{\frac{e_x}{e_k}}$$

and its stiffness in compression with

$$\frac{\partial P}{\partial e_x} = \frac{1}{2}\ \frac{P_k}{\sqrt{e_x\ e_k}}$$

On these premises the total sheet area to be added to the angle section is:

$$t\ s\ \frac{1+\nu\frac{e_y}{e_x}}{1-\nu^2}\ \frac{2b}{t} = t\ s\ \frac{1+\nu\frac{e_y}{e_x}}{1-\nu^2}\ \sqrt{\frac{e_k}{e_x}}$$

when determining the stress in the angle section, and

$$t\ s\ \frac{1+\nu\frac{e_y}{e_x}}{1-\nu^2}\ \frac{2b'}{t} = t\ s\ \frac{1+\nu\frac{e_y}{e_x}}{1-\nu^2}\ \frac{l}{2}\ \sqrt{\frac{e_k}{e_x}}$$

for the inertia moment of the angle section.

Illustrative Example

Top stringers of a flying-boat hull, figure 15

Given:

Compressive stress to be transferred by an angle section	P	= 450	kg
Inertia moment of section	J_p	= 0.15	cm^4
Area of section	F_p	= 0.4	cm^2
Distance of center of gravity	e	= 0.7	cm
Thickness of sheet	s	= 0.06	cm
Free buckling length of section (frame spacing)	l	= 60	cm

Since in this particular case the clamping by rivets is not complete, while the sheet strip lying between the two rivet rows is fairly well secured, we estimate the effective width to be equal to that of a sheet rigidly restrained in the section center.

The compression e_x of the sections is to be accompanied by their increased spacing e_y t so that $e_y = -0.1\ e_x$. For $\frac{e_y}{e_x} = -0.1$, the curve for clamped sheets in figure 3 discloses:

$$\sigma_k = 5.1\ E \left(\frac{s}{t}\right)^2 = 5.1 \times 700{,}000 \left(\frac{0.06}{20}\right)^2 = 32.2\ \frac{kg}{cm^2}$$

The compressive stress σ in sheet and section is obtained

by successive approximation. We first appraise $\sigma = 450$ kg/cm^2, whence $\sqrt{\frac{\sigma_k}{\sigma}} = 0.27$. From curve, figure 4, follows: $2\frac{b}{t} = 0.42$. Disregarding the transverse contraction cursorily - that is, putting the total effective width equal to 2b, the total effective cross-sectional area of sheet and angle section is

$$F = 0.4 + 0.42\ 20\ 0.06 = 9.9\ \text{cm}^2$$

and $\sigma = 500\ \frac{\text{kg}}{\text{cm}^2}$.

Owing to the omission of the transverse elongation, σ will lie slightly below $500\ \frac{\text{kg}}{\text{cm}^2}$. With $\sigma = 490$, it is:

$$\sqrt{\frac{\sigma_k}{\sigma}} = 0.256;\quad 2\frac{b}{t} = 0.41;\quad 2\frac{b_m}{t} = 0.41;\quad \frac{1 + \nu\frac{e_y}{e_x}}{1 - \nu^2} = 0.44$$

$$F = 0.925;\quad \sigma = 486\ \frac{\text{kg}}{\text{cm}^2}$$

The agreement is sufficiently exact.

The effective width with regard to the buckling load of the angle section now becomes $\frac{2b'}{t} = 0.256$, according to figure 4, and the effective sheet area is $F_m' = 0.3275$ cm^2. The center of pressure location is now as shown in figure 16. The calculation of the inertia moment of section plus effective sheet relative to this center of pressure gives:

$$I = 0.246\ \text{cm}^4$$

The Eulerian crippling load ($l = 60$ cm) becomes $P_k = 473$ kg; that is, the stipulated 450 kilograms are actually carried (fig. 16).

Centrical application of load is in the present example assured by the type of load division in the long sections extending over several bulkheads.

Lastly, we determine the maximum stress in the buckling sheet by superposing the flexural with the axial stresses.

Stress in compressive direction in the angle section:

$$\sigma_p = 486 \frac{kg}{cm^2} \quad ; \quad \text{for } \sqrt{\frac{e_k}{e_x}} = 0.256$$

becomes according to figure 11:

$$\frac{\sigma_{max}}{\sigma_{section}} = 1.3, \text{ that is, } \sigma_{max} = 630 \frac{kg}{cm^2}$$

DESCRIPTION OF EXPERIMENTS

The test material consisted of spring-hardened brass sheet, about 600x130mm of 0.1, 0.2, 0.4, and 0.6 mm gage which had been given a permanent elongation of 0.035 in the testing machine prior to clamping in order to void the stresses due to rolling. The elasticity moduli of these sheets were not in themselves necessary because the evaluation pertained solely to deformation comparisons. Still, one test was made which disclosed the elasticity modulus to be sufficiently constant for the stresses of the experimental range. In view of the unlike expansion coefficients of the testing material (brass) and the test equipment (steel) the temperature of the room and of the entire equipment had to be kept constant at $\pm 0.3^{\circ}$ so as to avoid appreciable thermal stress.

The test sheet was clamped in the machine with as little stress as possible. Then the sheet was subjected to longitudinal strain in (in general) both directions, causing the sheet to buckle. The setup also permitted the application of transverse loads on the test sheet.

To assure compression in longitudinal direction (figs. 17, 18) the sheet was clamped at the two longitudinal edges between two sets of duralumin rails B held by screws H. These clamping rails are pressed by slanting screws S against the very precisely machined guide surfaces of the very rigid guide rails K. The sheet is clamped at the upper and lower edges between cross pieces attached to the clamping rails. Then the screws S are temporarily loosened and the clamping rails and the test sheet are compressed in longitudinal direction. This is effected by tightening the screws R. The tensile stresses appearing as counter effect are taken up by separate ten-

sion members C, shown to right and left of the test sheet in figure 18. The compression of the clamping rails was recorded on self-manufactured Martens gages of 200 mm test length. The record was checked during overloading, yielding discrepancies of 1 percent as a rule, and 2 percent in one case.

The length of the cross beams D mounted on ball bearings to the two guide rails was adjustable, making it possible to subject the sheet also to elongations transverse to the longitudinal direction. With this in view, the weak center piece of the cross beams lying outside of the connecting line of the ball bearings was elastically twisted. The bending moment necessary for this was obtained by tightening of the turnbuckle E. The approach of the guide rails obtained was recorded on four dial gages M. This parallelogram guide system made direct application of transverse loads and the shifting of one guide rail relative to the other possible. For the experiments without transverse stress the weight of the guide rail, etc., was balanced by a counter weight N.

The slope of the buckled sheet was read on the slope gage, (figs. 19, 20) whose deflection was indicated by a glass pointer with metal tip on a finely graduated glass scale. Both slope gage and glass scale were mounted on a small tube which was easily shifted toward the sheet.

As this tube, together with the slope gage, pivoted exactly through 90° it was possible to record the slope of the sheet in perpendicular and horizontal direction $\left(\frac{\partial w}{\partial x}; \frac{\partial w}{\partial y}\right)$. To assure reaching the individual test points, the entire setup was mounted on a slide which was horizontally and vertically adjustable.

Altogether 29 different loading conditions were measured, 18 of them with constant spacing of stiffening sections ($e_y = 0$), besides 11 tests with transverse elongations e_y of certain magnitude. The average number of slope measurements in each loading condition was 600.

Figure 21 illustrates the measured slopes in longitudinal (x) direction for a certain sheet. The figures seen near the curves denote the distance of the curves from the edge. One can see the divergence from the sinusoidal course of the slopes at the edge caused by thrust in intermediate wrinkles.

APPENDIX

Calculation of mean stresses from the recorded deformations*.- In the coordinate system, figure 22, ξ, η, and w represent the displacement coordinates, and x and y the running sheet coordinates.

Notation

t, width of sheet

l, length of integration range in x direction

σ_x σ_y τ, stresses in center of sheet,

$\bar{\sigma}_x$ $\bar{\sigma}_y$ $\bar{\tau}$, mean values of stresses, averaged in x direction

ϵ_x ϵ_y γ, deformation quantities in central area of sheet

e_x e_y g, mean deformations of total field

$$e_x = \frac{\xi_e - \xi_o}{l}; \quad e_y = \frac{\eta_t - \eta_o}{t}; \quad g = \frac{\xi_t - \xi_o}{t}$$

σ_{x_B} σ_{y_B} τ_B, stresses existing in the field deformed with e_x, e_y, g in case the buckling is prevented.

$\nu = \frac{1}{m}$ transverse contraction factor.

$$J^x_{xx} = \frac{1}{2l}\int_0^l \left(\frac{\partial w}{\partial x}\right)^2 dx; \quad J^x_{yy} = \frac{1}{2l}\int_0^l \left(\frac{\partial w}{\partial y}\right)^2 dx;$$

$$J^x_{xy} = \frac{1}{l}\int_0^l \left(\frac{\partial w}{\partial x}\cdot\frac{\partial w}{\partial y}\right) dx;$$

$$J^{xy}_{xx} = \frac{1}{2\,l\,t}\int_0^t\int_0^l \left(\frac{\partial w}{\partial x}\right)^2 dx\,dy;$$

$$J^{xy}_{yy} = \frac{1}{2\,l\,t}\int_0^t\int_0^l \left(\frac{\partial w}{\partial y}\right)^2 dx\,dy.$$

---

*In view of the report on the experiments with transverse stresses in the sheet, which is to follow, the necessary formulas are repeated here.

For every point of the sheet (cf. Föppl: Drang und Zwang):

$$\frac{\sigma_x}{E} - \frac{\sigma_y}{m\,E} = \epsilon_x = \frac{\partial \xi}{\partial x} + \frac{1}{2}\left(\frac{\partial w}{\partial x}\right)^2 \tag{7a}$$

$$\frac{\sigma_y}{E} - \frac{\sigma_x}{E\,m} = \epsilon_y = \frac{\partial \eta}{\partial y} + \frac{1}{2}\left(\frac{\partial w}{\partial x}\right)^2 \tag{7b}$$

$$\frac{\tau}{G} = \gamma = \frac{\partial \xi}{\partial y} + \frac{\partial \eta}{\partial x} + \frac{\partial w}{\partial x}\frac{\partial w}{\partial y} \tag{7c}$$

or, solved according to the stresses:

$$(1 - \nu^2)\,\frac{\sigma_x}{E} = \frac{\partial \xi}{\partial x} + \frac{1}{2}\left(\frac{\partial w}{\partial x}\right)^2 + \nu\left[\frac{\partial \eta}{\partial y} + \frac{1}{2}\left(\frac{\partial w}{\partial y}\right)^2\right] \tag{8}$$

$$(1 - \nu^2)\,\frac{\sigma_y}{E} = \frac{\partial \eta}{\partial y} + \frac{1}{2}\left(\frac{\partial w}{\partial y}\right)^2 + \nu\left[\frac{\partial \xi}{\partial x} + \frac{1}{2}\left(\frac{\partial w}{\partial x}\right)^2\right] \tag{9}$$

$$\frac{\tau}{G} = \frac{\partial \xi}{\partial y} + \frac{\partial \eta}{\partial x} + \frac{\partial w}{\partial x}\frac{\partial w}{\partial y} \tag{10}$$

Formulating the mean values by integration over x

$$(1 - \nu)^2\,\frac{\overline{\sigma_x}}{E} = e_x + J^x_{xx} + \nu\left(\frac{1}{e}\int_0^l \frac{\partial \eta}{\partial y}\,\partial x + J^x_{yy}\right) \tag{11}$$

$$(1 - \nu^2)\,\frac{\overline{\sigma_y}}{E} = \frac{1}{e}\int_0^l \frac{\partial \eta}{\partial y}\,dx + J^x_{yy} + \nu\,(e_x + J^x_{xx}) \tag{12}$$

$$\frac{\overline{\tau}}{G} = \frac{1}{e}\int_0^l \frac{\partial \eta}{\partial x}\,dx + \frac{1}{e}\int_0^l \frac{\partial \xi}{\partial y}\,dx + J^x_{xy} \tag{13}$$

We then eliminate $\frac{1}{e}\int_0^l \frac{\partial \eta}{\partial y}\,dx$ from equations (11) and (12):

$$\frac{\overline{\sigma_x}}{E} = e_x + J^x_{xx} + \nu \frac{\overline{\sigma_y}}{E} \tag{14}$$

By integration over y equation (13) gives:

$$\frac{\tau}{G} = y + J^{xy}_{xy} \tag{15}$$

We average equation (12) over y and write the value for $\frac{\nu}{E}\overline{\sigma_y}$ in equation (14):

$$\overline{\sigma_x} = \frac{E}{1 - \nu^2}\left[e_x + \nu\left(e_y + J^{xy}_{yy}\right) + r^2 J^{xy}_{xx}\right] + E J^x_{xx} \tag{16}$$

In order to determine the total load absorbed by the sheet, this equation must be multiplied by the sheet thickness and integrated over y from o to t:

$$P = s\int_o^t \overline{\sigma_x}\, d x = \frac{E s t}{1 - \nu^2}\left[e_x + \nu\left(e_y + J^{xy}_{yy}\right) + J^{xy}_{xx}\right] \tag{17}$$

As the effective width b is referred to the stress σ_{x_B} existing in the sheet at equal e_x, e_y when buckling is prevented, it is

$$b = \frac{P}{2\,\sigma_{x_B}\, s}$$

For the case $e_y = 0$ it becomes

$$\sigma_{x_B} = \frac{e_x E}{1 - \nu^2}$$

that is,

$$b = \frac{P(1 - \nu^2)}{2\, E\, \sigma_{x_B}\, s} \tag{18}$$

All the quantities on the right-hand side of (17) are obtained from the actual measurements.

The slopes $\frac{\partial w}{\partial x}$ and $\frac{\partial w}{\partial y}$ necessary to define the integral values J^{xy}_{xx} and J^{xy}_{yy} were known only at the individual test points. The latter were chosen so closely together that the integral was replaceable by sums without appreciable error.

The finite distance of the points of the slope gage (5 mm) causes an instrumental error which in first approximation is proportional to the second derivation of the slope $\left(\text{for example } \frac{\partial^3 w}{\partial x^3}\right)$. To correct this error this second derivation was determined from the recorded slopes in the adjacent points.

An analysis of the equilibrium of the mean sheet fiber revealed a possibility of checking the longitudinal elongation e_x recorded with the Martens instrument. The process is briefly as follows:

The form of the sheet was approximately represented by

$$\frac{\partial w}{\partial x} = \bar{\varphi}_o \sin \frac{\pi x}{l} (1 - a y^2 - b y^4) \qquad (19)$$

which actually is quite correct in the vicinity of the mean fiber; y is measured from the center of the sheet. The values $\bar{\varphi}_o$, a, and b can be obtained from the values J^x_{xx} known from the tests for $y = 0$, $y = y_1$; $y = y_2$; l itself is known from the measurement direct.

We proceed from the equilibrium condition of a part of the median fiber in the form:

$$\sigma_x \, s \, \frac{\partial^2 w}{\partial x^2} + \sigma_y \, s \, \frac{\partial^2 w}{\partial y^2} = B \left(\frac{\partial^4 w}{\partial x^4} + 2 \frac{\partial^4 w}{\partial x^2 \, \partial y^2} + \frac{\partial^4 w}{\partial y^4} \right)$$

There are no shear stresses for reasons of symmetry. B is the bending stiffness of the sheet. This assumed function inserted in equation (19) and with $y = 0$, voids $\bar{\varphi}_o \cos \frac{\pi x}{l}$, so that all terms become free of x and y.

In this relation between σ_x and σ_y these two quantities

can be replaced by the mean values $\overline{\sigma}_x$ and $\overline{\sigma}_y$, after which e_x can be obtained from equations (14) and (16). This method was followed for checking the entire test measurements. For $\frac{e_x}{e_k} < 15$ the data were at variance with those of the Martens instruments. The discrepancy between the assumed and the actual sheet form noticeable at the higher powers of y in equation (19) are more pronounced. For $\frac{e_x}{e_k} > 15$ the agreement is fairly close (2 percent discrepancy at the most). For very high $\frac{e_x}{e_k}$ a very accurate knowledge of e_x is necessary with regard to the determination of the effective width b according to (17) or (18). And here the last described method gives very reliable and accurate data for e_x.

Dimensional Analysis

The equilibrium on a rectangular sheet element is defined by

$$K s^2 \Delta \Delta w = \frac{\sigma_x}{E} \frac{\partial^2 w}{\partial x^2} + \frac{2 \tau_{xy}}{E} \frac{\partial^2 w}{\partial x \partial y} + \frac{\sigma_y}{E} \frac{\partial^2 w}{\partial y^2}$$

$$\frac{\partial \sigma_x}{\partial x} + \frac{\partial \tau_{xy}}{\partial y} = 0$$

$$\frac{\partial \sigma_y}{\partial y} + \frac{\partial \tau_{xy}}{\partial x} = 0$$

There are six more equations for the deformation and stress quantities:

$$\frac{\sigma_x}{E} = \frac{1}{1 - \nu^2} (\epsilon_x + \nu \epsilon_y)$$

$$\frac{\sigma_y}{E} = \frac{1}{1 - \nu^2} (\epsilon_y + \nu \epsilon_x)$$

$$\frac{\tau}{E} = \frac{m}{2(m + 1)} \gamma$$

$$\epsilon_x = \frac{\partial \xi}{\partial x} + \frac{1}{2}\left(\frac{\partial w}{\partial x}\right)^2$$

$$\epsilon_y = \frac{\partial \eta}{\partial y} + \frac{1}{2}\left(\frac{\partial w}{\partial y}\right)^2$$

$$\gamma = \frac{\partial \xi}{\partial y} + \frac{\partial \eta}{\partial x} + \frac{\partial w}{\partial x}\frac{\partial w}{\partial y}$$

These nine equations define the nine dependent variables σ_x σ_y τ; ϵ_x ϵ_y γ; ξ η w with respect to coordinates x and y, as well as relative to the dimensional quantities s and t and, with respect to the defined e_x, g, e_y, the limiting conditions

for $-\infty < x < +\infty$ and for $y = 0$, $y = t$ $w = 0$, $\frac{\partial w}{\partial y} = 0$

for $y = 0$ $\quad \zeta = e_x x \quad \eta = 0$

for $y = t$ $\quad \zeta = e_x s + g t \quad \eta = e_y t$

The quantities s and t can be separately eliminated when

$$\frac{\sigma_x t^2}{E s^2} \quad \frac{\sigma_y t^2}{E s^2} \quad \frac{\tau t^2}{E s^2}, \quad \epsilon_x \left(\frac{t}{s}\right)^2 \quad \epsilon_y \left(\frac{t}{s}\right)^2 \quad \gamma \left(\frac{t}{s}\right)^2 \quad \xi \frac{t}{s^2} \quad \eta \frac{t}{s^2} \quad \frac{w}{s}$$

is chosen as dependent variable, i.e., by writing in the new equations and in the limiting conditions $\frac{x}{t}$ and $\frac{y}{t}$ as independent variables. Then the limiting conditions, for example, become

for $-\infty < \frac{x}{t} < +\infty$ and for $\frac{y}{t} = 0$ and $\frac{y}{t} = 1$

$$\frac{w}{s} = 0 \qquad \frac{\partial \frac{w}{s}}{\partial \frac{y}{t}} = 0$$

for $\frac{y}{t} = 0$ $\quad \frac{\xi t}{s^2} = \frac{e_x t^2}{s^2}\frac{x}{t} \quad \frac{\eta t}{s^2} = 0$

for $\frac{y}{t} = 1$ $\quad \frac{\xi\, t}{s^2} = \frac{e_x\, t^2}{s^2}\frac{x}{t} + \frac{g}{e_x}\frac{e_x\, t^2}{s^2}\frac{\eta\, t}{s^2} - \frac{e_y}{e_x}\frac{e_x\, t^2}{s^2}$

The newly chosen dependent variables then depend, apart from $\frac{x}{t}$, $\frac{y}{t}$ on the quantities $e_x\left(\frac{t}{s}\right)^2$, $\frac{e_y}{e_x}$, $\frac{g}{e_x}$ defining the limiting conditions. In this nondimensional form, the effective width, that is, $\frac{b}{t}$, which is not dependent on the coordinates, can therefore be dependent only on the latter quantities, that is:

$$b = t\, C, \text{ whereby } \quad C = C\left[e_x\left(\frac{t}{s}\right)^2, \frac{e_y}{e_x}, \frac{g}{e_x}\right]$$

which, after dividing both sides by $\sqrt{\frac{e_x\, t^2}{s^2}}$, can be written as

$$\frac{b}{s}\sqrt{e_x} = C_1, \quad \text{whereby} \quad C_1 = C_1\left[e_x\left(\frac{t}{s}\right)^2, \frac{e_y}{e_x}, \frac{g}{e_x}\right]$$

Translation by J. Vanier
National Advisory Committee
for Aeronautics.

REFERENCE

1. Schnadel, G.: Knickung von Schiffplatten, Werft Reederei Hafen, vol. 11, nos. 22 and 23, 1930.

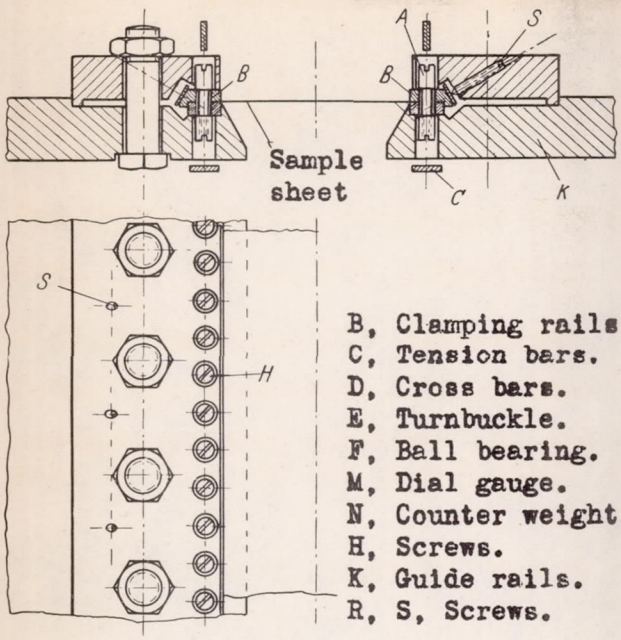

B, Clamping rails.
C, Tension bars.
D, Cross bars.
E, Turnbuckle.
F, Ball bearing.
M, Dial gauge.
N, Counter weight.
H, Screws.
K, Guide rails.
R, S, Screws.

Figure 17

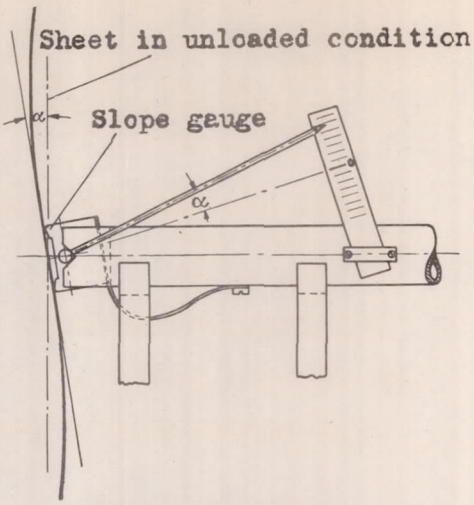

Figure 19:- Gauge.

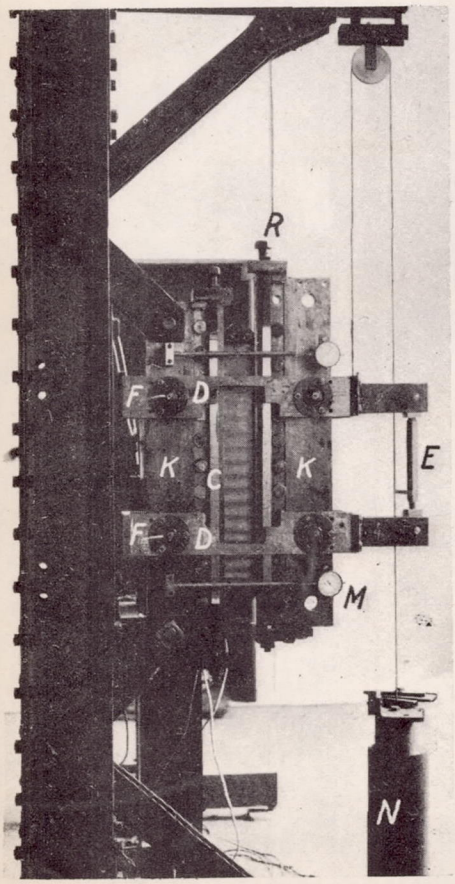

Figure 17,18:- Mounting of specimen sheet.

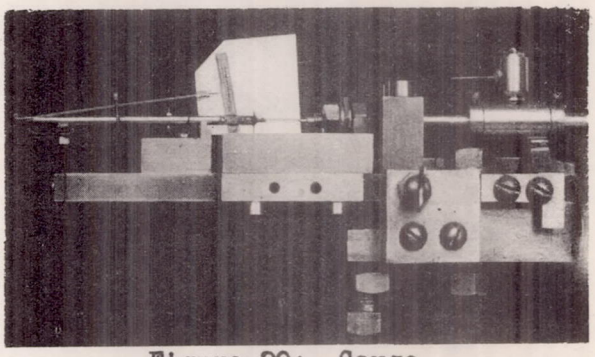

Figure 20:- Gauge.

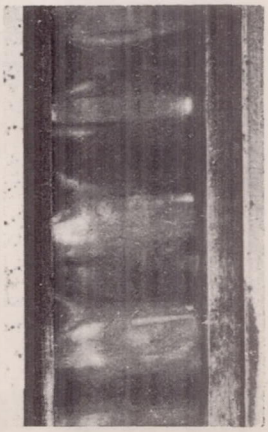

Figure 1:- Buckled sheet; buckling load exceeded about 40 times.

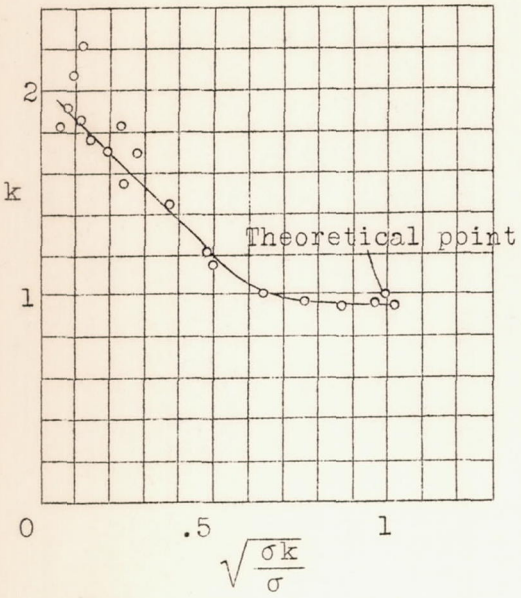

Figure 2.- Factor k versus amount of exceeded buckling load.

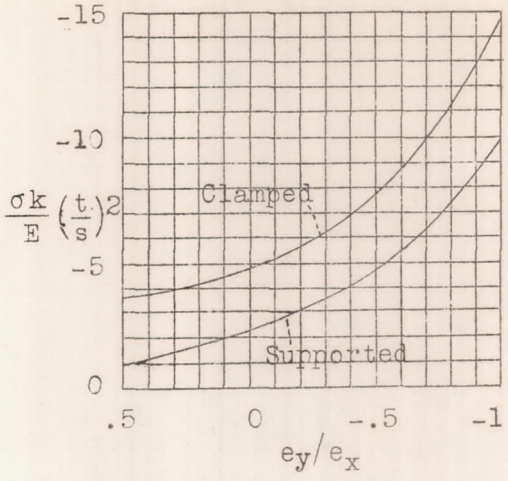

Figure 3.- Theoretical values of buckling load of sheet; s = sheet thickness, E = Young's modulus, t = spacing of edge stiffeners.

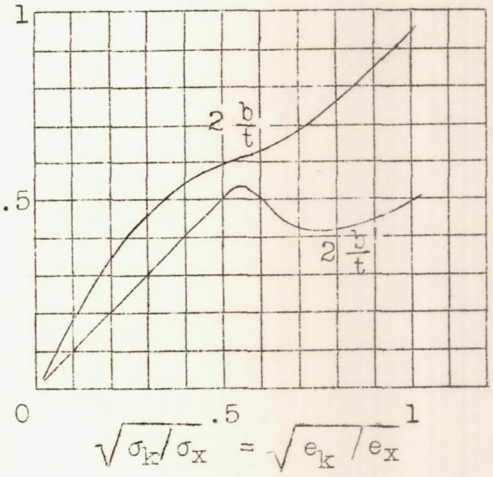

Figure 4.- Experimentally defined curves for computing the effective width with regards to the load taken up by the sheet ($2\frac{b}{t}$ to be written in equation (1)) and with regards to the width of the sheet strip to be considered in the calculation of the buckling load of the angle section ($2\frac{b'}{t}$ to be written in equation (1)).

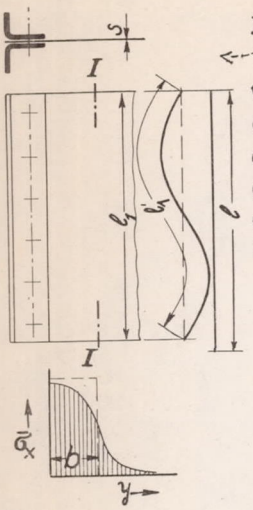

Figure 5.- Owing to wrinkling the compressive stress drops at some distance from the edge stiffener to nearly zero.

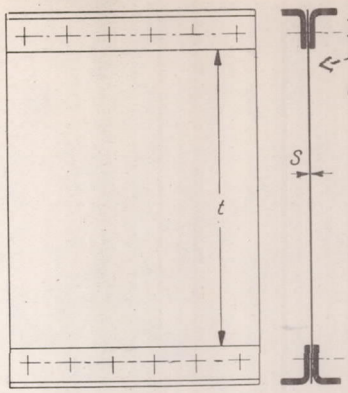

Figure 6.- Sheet with edge stiffeners.

Figure 9.- Compression taken up by the sheet.

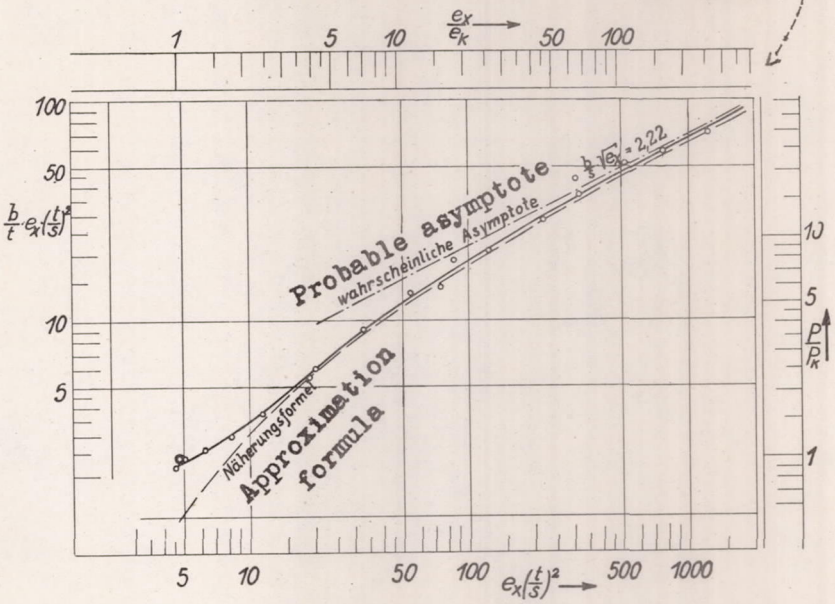

Figure 11.- The compressive stress in the buckled sheet together with the bending stress due to wrinkling, forms a resultant stress which attains its maximum in the sheet center when the buckling is slightly exceeded and near the edge stiffener if the buckling load is largely exceeded.

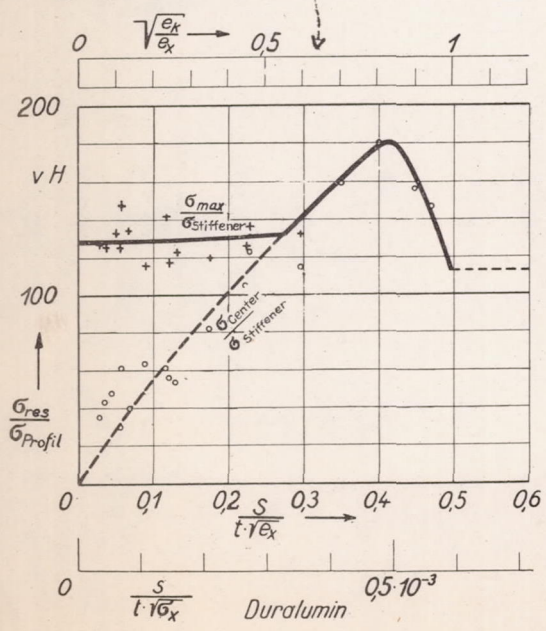

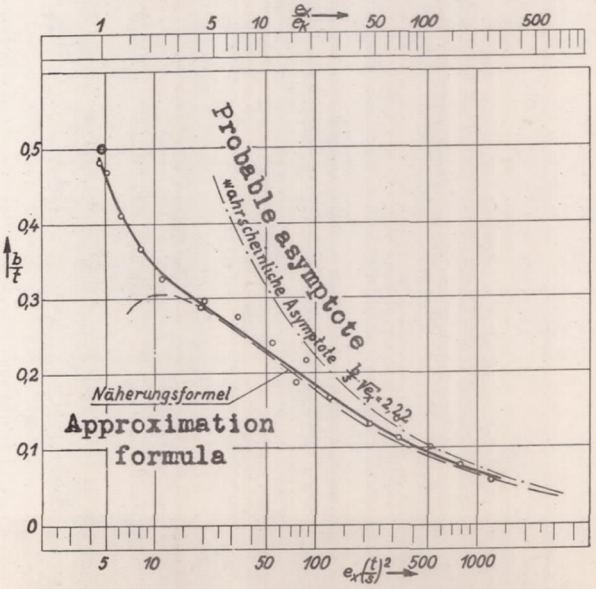

Figure 7.- Illustration of the test data for effective width.

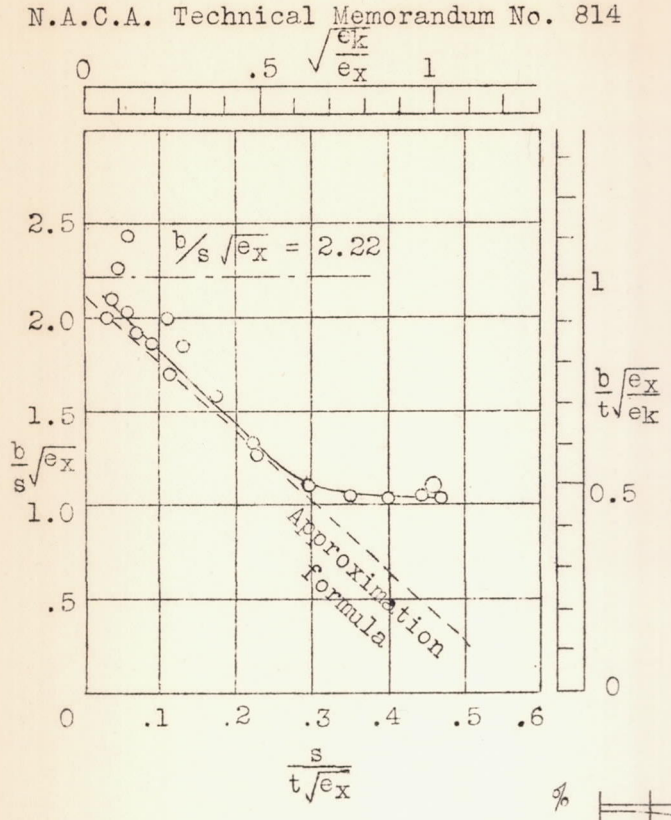

Figure 8.- Illustration of the test data for effective width.

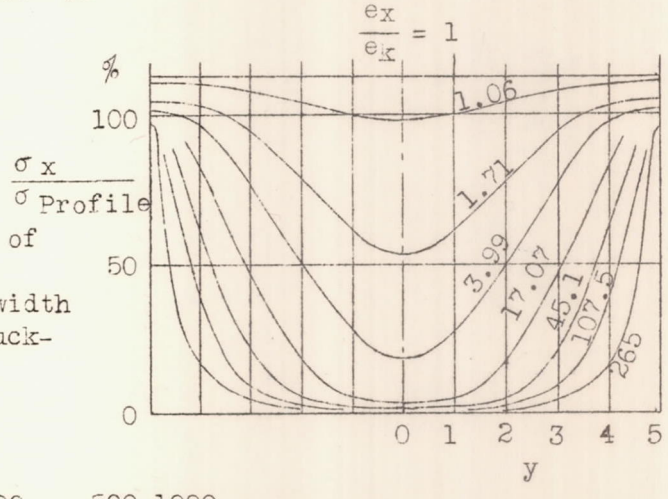

Figure 10.- Distribution of compressive stresses over the sheet width for varyingly exceeded buckling load.

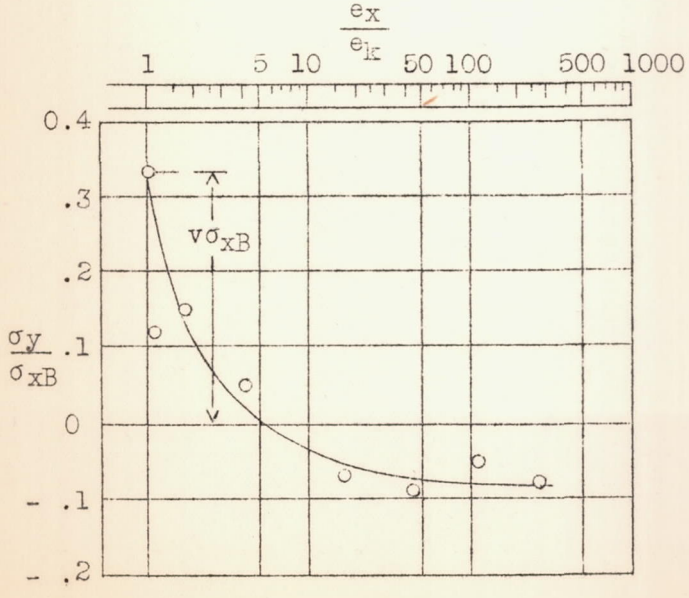

Figure 12.- Stresses transverse to direction of compression.

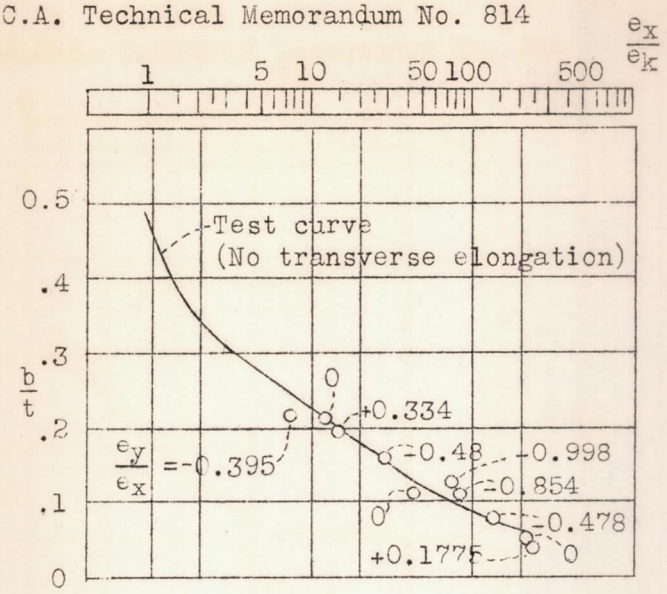

Figure 13.- Effective width when elongations transverse to compressive direction are prevalent.

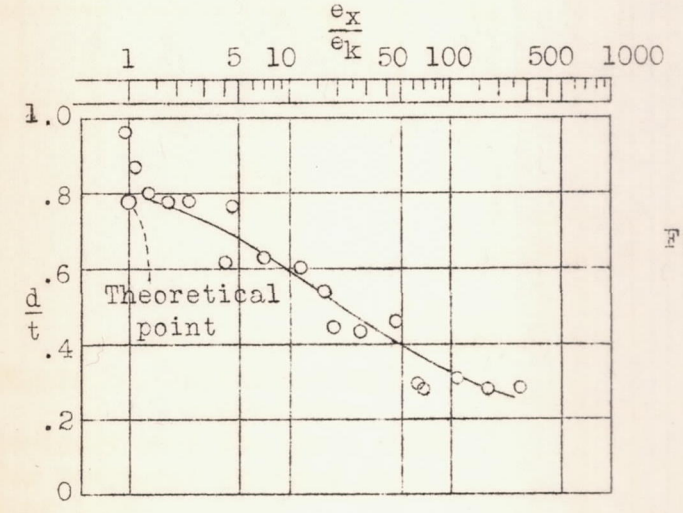

Figure 14.- Length of buckle.

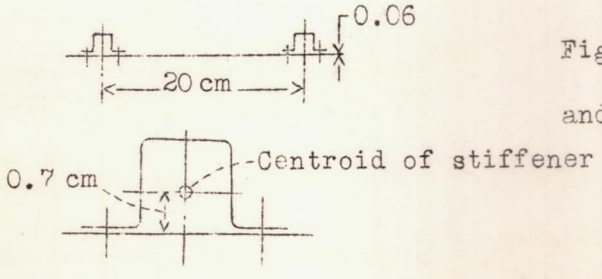

Figure 15.- Dimensions of sheet and angle section.

A Width relative to buckling load, 5.45 cm.
B " " " force, 8.8 cm

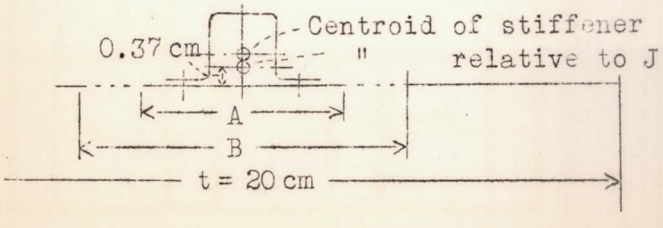

Figure 16.- Effective width with regard to load absorbed and width of sheet strip to be considered for the calculation of the buckling load of the edge stiffener.

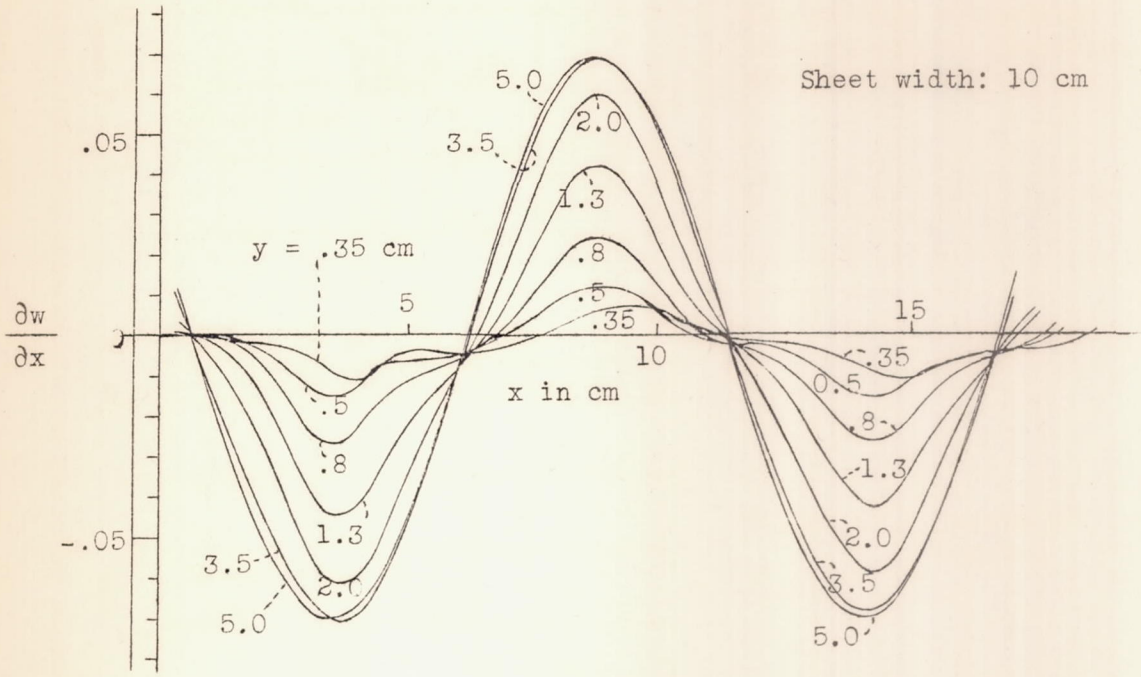

Figure 21.- Measured slopes for buckling load exceeded 15 times.

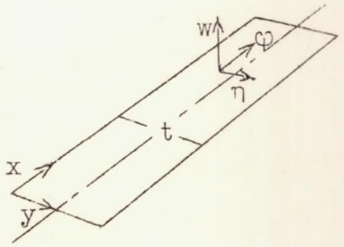

Figure 22.- Coordinate system.